

Singularity removal in a quantum effective evolution of the Mixmaster cosmological model

Héctor Hugo Hernández Hernández¹, Gustavo Alejandro Sánchez Herrera²
email: ¹hhernandez@uach.mx, ²cbi2233805002@xanum.uam.mx

January 9, 2024

^{1,2}*Universidad Autónoma de Chihuahua, Facultad de Ingeniería,
Nuevo Campus Universitario, Chihuahua 31125, México.*

Abstract

In this work we analyze the evolution of the quantum Mixmaster cosmological model within an effective approach. In particular, we study the behaviour of the scale factor and anisotropies of the theory, and determine how it deviates from its classical counterpart due to quantum back-reaction. Remarkably, we determine that the effective evolution avoids the initial singularity. The semiclassical dynamic of the system is obtained from a Hamiltonian in an extended phase space, whose classical position and momentum variables are the expectation values of the corresponding quantum operators, as well as of quantum dispersions and correlations of the system, and is in this framework that we obtain semiclassical one-particle trajectories.

Keywords: Effective Hamiltonian. Bianchi IX model, Mixmaster model

1 Introduction.

In the mid-20th century Evgeny Lifshitz discovered that as the universe shrinks to regions of space close to the initial singularity, spacetime is no longer isotropic [1]. Because of this, the interest in anisotropic cosmological models increased considerable during the past years [2, 3, 4, 5]. One of the most prominent results of these investigations is the BKL conjecture, stating that, in a general way, it is possible to neglect the matter terms near the initial singularity because, for them, time derivatives are dominant over those with spatial derivatives; the dynamics in this case is described by the Bianchi IX model [6]. In recent years, a great variety of studies of anisotropic models of the universe, based on this conjecture, have been carried out [7, 8, 9].

The most general anisotropic homogeneous model of the universe, based on the BKL conjecture, is the Mixmaster [10]. It describes the behavior of the universe near the initial singularity. The universe is treated as a point particle moving through the anisotropies space, subject to a time-dependent potential [11]. The studies carried out on the classic Mixmaster model have shown that it is not only singular, but also has a chaotic behavior close to the initial singularity [12, 13, 14], therefore, a quantization scheme is introduced in the anticipation of mitigating these issues. Among the most interesting approaches in the analysis of these quantum cosmological models are effective quantization schemes based on loop quantum gravity [15], and effective polymeric quantum mechanics [16], showing that the initial singularity is removed, and the chaos present in the theory is reduced [17] This shows the importance of effective quantization approaches in analyzing complex cosmological models, as the ones mentioned above.

Quantum effective methods in quantum mechanics allow us to obtain an approximate solution of the whole system. In particular, momenta quantum mechanics reduces quantum systems to semiclassical ones, where the dynamics is obtained from an effective Hamiltonian in an extended phase space [18]. One of the most prominent features of this method is that the notion of individual particle-trajectories is recovered, a characteristic not existing in usual quantum mechanics. This trajectories describe the evolution of expected values of position and momentum operators, and of the (infinite many) quantum dispersions. The versatility of application of this method has allowed the study of a broad spectrum of quantum systems, ranging from the relatively simple phenomenon of quantum tunneling [19], to models of quantum cosmology [20, 21, 22].

In this work we obtain a system of effective equations of motion for spatial anisotropies and the scale factor of the Mixmaster model, once we determine the effective extended Hamiltonian. The interaction of the several degrees of freedom of the system is encoded in an effective potential, obtained in a direct way. In section 2 we review the more general aspects of the classical Mixmaster model and perform a canonical transformation to explicitly express the Hamiltonian of the theory as a kinetic plus potential term. In section 3 we provide the formalism of momenta quantum mechanics, and we apply this to the Mixmaster model in order to obtain the effective dynamics of the system. Finally, in section 4 the semiclassical evolution is analyzed.

2 Classical Mixmaster model

The interest in investigating the Mixmaster model lies in its representation as a general solution to Einstein's equations near the initial singularity [23]. Furthermore, various studies have been conducted that provide substantial evidence supporting the BKL conjecture [24, 25, 26]. We will analyze the quantum model with an effective prescription of quantum mechanics, so we start with a discussion of the classical model.

The most general anisotropic cosmological model is the Bianchi IX, whose metric is given by [11]

$$ds^2 = -N^2(t)dt^2 + g_{ij}(t)\sigma_i\sigma_j, \quad (1)$$

where N is the lapse function, and σ are differential forms of the three-sphere [27]

$$\begin{aligned} \sigma_1 &= \cos(\psi)d\theta + \sin(\psi)\sin(\theta)d\phi, \\ \sigma_2 &= \sin(\psi)d\theta - \cos(\psi)\sin(\theta)d\phi, \\ \sigma_3 &= d\psi + \cos(\theta)d\phi. \end{aligned}$$

In particular, the metric g_{ij} can be written in terms of the Misner parameters α , and β such that (1) is

$$ds^2 = -N^2 dt^2 + e^{2\alpha}(e^{2\beta})_{ij}\sigma^i\sigma^j, \quad (2)$$

where α is the parameter determining the volume of the universe, and β_{ij} is a null trace matrix $\text{tr}(\beta_{ij}) = 0$ containing the spatial anisotropies. The components of the matrix β_{ij} satisfy the following equations [28]

$$\begin{aligned} \beta_{11} &= \beta_+ + \sqrt{3}\beta_-, \\ \beta_{22} &= \beta_+ - \sqrt{3}\beta_-, \\ \beta_{33} &= -2\beta_+. \end{aligned} \quad (3)$$

On the other hand, the square root of the determinant of the metric $\sqrt{\det(g_{ij})}$ from eq. (2) allow us to identify the volume of the universe as the scale factor $a(t)$ in terms of the parameter α [11]

$$a(t) = \sqrt{\det(g_{ij})} = \exp(3\alpha). \quad (4)$$

The relation between the parameters α, β_+, β_- with the scale factor $a(t)$ is [28]

$$\begin{aligned} \alpha(t) &= \frac{1}{3}\ln(a(t)), \\ \beta_+(t) &= \frac{1 - P_3}{2}\alpha(t), \\ \beta_-(t) &= \sqrt{3}(P_1 - P_2)\alpha(t), \end{aligned} \quad (5)$$

where P_i are the Kasner coefficients. For instance, to describe a universe that expands in two directions, and contracts in the other, the coefficients P_i are $P_1 = P_3 = 2/3$, and $P_2 = -1/3$ [29]. The equation (4) shows that as $\alpha \rightarrow -\infty$, $a(t) \rightarrow 0$, which corresponds to the initial singularity

When the Hamiltonian formulation for the Bianchi IX model is introduced, the resulting model is the Mixmaster. Its dynamics is determined by a Hamiltonian \mathcal{H} , which is obtained through the variation of the following action [28]

$$I = \int dt \left(p_\alpha \dot{\alpha} + p_+ d\dot{\beta}_+ + p_- d\dot{\beta}_- - N\mathcal{H} \right), \quad (6)$$

where p_α , and p_\pm are the conjugate momenta of α and β_\pm [22]. \mathcal{H} is defined as

$$\mathcal{H} = \frac{k}{3(8\pi)^2} e^{-3\alpha} (-p_\alpha^2 + p_+^2 + p_-^2 + \mathcal{V}), \quad (7)$$

with

$$\mathcal{V} = \frac{3(4\pi)^2}{k^2} e^{4\alpha} V(\beta_\pm), \quad (8)$$

where $k = 8\pi G$ and V is the potential. Its particular form for the Bianchi IX model [30] is the following

$$V(\beta_\pm) = e^{-8\beta_+} - 4e^{-2\beta_+} \cosh(2\sqrt{3}\beta_-) + 2e^{4\beta_+} [\cosh(4\sqrt{3}\beta_-) - 1]. \quad (9)$$

This potential is a function of anisotropies β_+ , β_- , and is graphically represented by equilateral triangles that evolve in time as shown in the figure 1. In general, \mathcal{H} contains the physics of all the Bianchi universes in the potential term \mathcal{V} from the equation (8), where to each Bianchi model corresponds a different equipotential line [23].

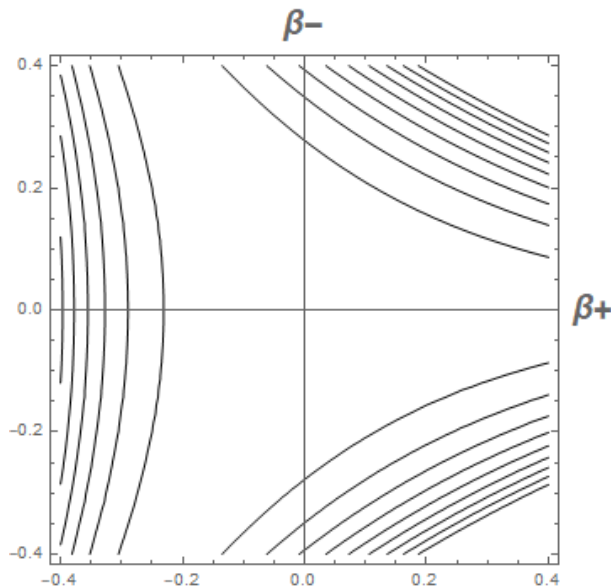


Figure 1: Parametric representation of the Mixmaster potential. The equipotential lines shows how the potential evolve in time.

The dynamics is obtained through the variation of (6) with respect to each of the variables. The variation with respect to the lapse function N generates the Hamiltonian constraint $\mathcal{H} = 0$. Solving for p_α we have

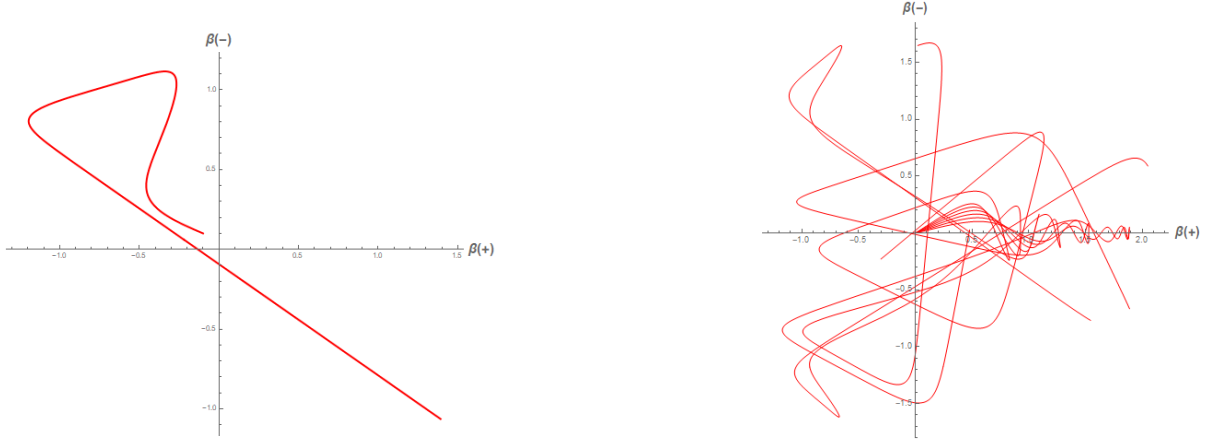
$$-p_\alpha = H_{IX} = \sqrt{p_+^2 + p_-^2 + \mathcal{V}}. \quad (10)$$

From this expression one obtains the dynamics of the universe represented as a point particle subject to a variable potential in the space of anisotropies β_+ , and β_- . Each of the classical variables evolves with respect to the parameter α . Close to the initial singularity, it is possible to show that the particle moves twice as fast as the separation movement of the potential walls, and then it experiences consecutive reflections as the volume of the universe decreases [28].

Given the Hamiltonian in (10), and using the potential $V(\beta_\pm)$ from (9), we get the following set of classical equations of motion for the Mixmaster model

$$\begin{aligned} \dot{\beta}_+ &= \frac{p_+}{H_{IX}}, \\ \dot{\beta}_- &= \frac{p_-}{H_{IX}}, \\ \dot{p}_+ &= 4 \frac{3(4\pi)^2}{k^2 H_{IX}} e^{4\alpha} \left[e^{-8\beta_+} - e^{-2\beta_+} \cosh(2\sqrt{3}\beta_-) \right. \\ &\quad \left. - e^{4\beta_+} (\cosh(4\sqrt{3}) - 1) \right], \\ \dot{p}_- &= 4\sqrt{3} \frac{3(4\pi)^2}{k^2 H_{IX}} e^{4\alpha} \left[e^{-2\beta_+} \sinh(2\sqrt{3}\beta_-) \right. \\ &\quad \left. - e^{4\beta_+} \sinh(4\sqrt{3}) \right]. \end{aligned} \quad (11)$$

This is a highly non-linear, coupled system for the classical anisotropies and their momenta, so we solve it numerically. The evolution obtained is shown in figure 2. Figure 2a shows that the trajectory of the universe experience reflections at the potential barriers, while in the figure 2b we can see the chaotic behaviour of the classical system for different given trajectories. As the universe approaches the initial singularity, the reflections of the particle with the potential barriers decrease, and the trajectory of the universe behaves as a straight line in space of anisotropies [17], while the parameter α tends to minus infinity. The initial singularity corresponds to $|\beta_{\pm}| \rightarrow \infty$.

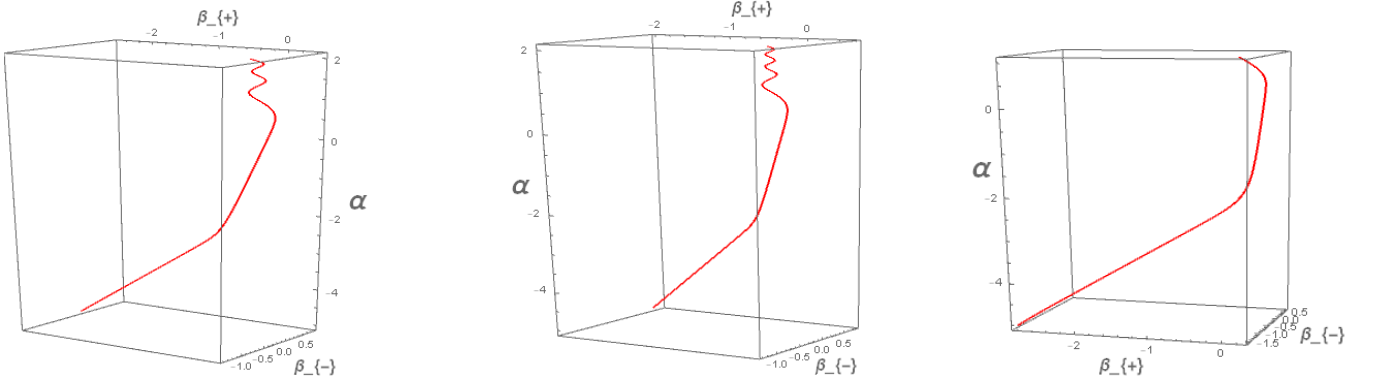


(a) The initial conditions are $\beta_+ = -0.1$, $\beta_- = 0.1$, $p_{\beta_+} = -3$, $p_{\beta_-} = 1.28$. The value of $V(\beta_+, \beta_-)$ is of the order of $\exp\{-4\alpha\}$

(b) The initial conditions are $\beta_+ = \beta_- = 0$, $p_{\beta_+} = 100$, $p_{\beta_-} = 8$. The value of $V(\beta_+, \beta_-)$ is of the order of $\exp\{-1.2\alpha\}$.

Figure 2: Trajectory of the particle in space (β_+, β_-) for different values of $V(\beta_+, \beta_-)$. It is shown how the temporal dependence of $V(\beta_+, \beta_-)$ results in reflection in different equipotential lines.

In figure 3 those trajectories are plotted in three-dimensional space $(\beta_+, \beta_-, -\alpha)$.



(a) The initial conditions are $x(0) = 0.1$, $y(0) = 0.1$, $px(0) = -60$, $py(0) = 200$.

(b) The initial conditions are $x(0) = 0.1$, $y(0) = 0.1$, $px(0) = -80$, $py(0) = 200$.

(c) The initial conditions are $x(0) = 0.1$, $y(0) = 0.1$, $px(0) = -30$, $py(0) = 200$.

Figure 3: Trajectory of the particle in space $(\beta_+, \beta_-, -\alpha)$. The pictures shows that for any initial condition, as time goes backwards, α goes to $-\infty$, and the classical singularity is reached.

Applying the canonical transformations $q = \exp\{(3/2)\alpha\}$, $p = \frac{3}{2} \exp\{-(3/2)\alpha\} p_\alpha$ for the variables α , and p_α , and $p'_+ = p_+/q$, $\beta'_+ = \beta_+q$, $p'_- = p_-/q$, $\beta'_- = \beta_-q$ for the anisotropies and their momenta, the Hamiltonian constraint (7) reduces to the following [31]

$$\mathcal{K} = -\frac{9}{4}p^2 + p'^2_+ + p'^2_- + \frac{3(4\pi)^4}{k}q^{2/3}V(q, \beta'_+, \beta'_-), \quad (12)$$

where the potential $V(q, \beta'_+, \beta'_-)$ is given by

$$V(q, \beta'_+, \beta'_-) = e^{-\frac{8\beta'_+}{q}} - 4e^{-\frac{2\beta'_+}{q}} \cosh\left(\frac{2\sqrt{3}\beta'_-}{q}\right) + 2e^{\frac{4\beta'_+}{q}} \left[\cosh\left(\frac{4\sqrt{3}\beta'_-}{q}\right) - 1 \right]. \quad (13)$$

In the isotropic limit $\beta'_+ = \beta'_- = p'_+ = p'_- = 0$, the potential $V(\beta_+, \beta_-, q)$ is a negative constant with value $V(\beta_+, \beta_-, q) = -3$. Then (12) becomes

$$\mathcal{K}_{iso} = \frac{1}{4}p^2 + 32\pi^3 q^{2/3}. \quad (14)$$

When we consider the isotropic part of the system, (12) reduces to (14), which has only one degree of freedom. From this, the classical equations of motion for q and p are

$$\begin{aligned} \dot{q} &= \frac{p}{2}, \\ \dot{p} &= -\frac{64}{3}\pi^3 q^{-1/3}. \end{aligned} \quad (15)$$

Since $q = \exp\{(3/2)\alpha\}$, from (4) we know that $q = \sqrt{a}$. Therefore, $q \rightarrow 0$ implies that $a \rightarrow 0$ and $\text{Log}(q) \rightarrow -\infty$, that corresponds to the initial singularity. In figure 4 we show the relation between $\text{Log}(q)$ and p .

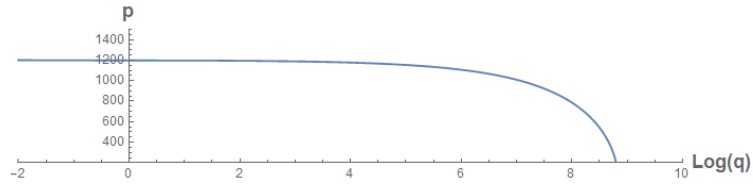


Figure 4: Plot between q and p . Since $q = \exp\{(3/2)\alpha\}$, the initial singularity occurs when the $\text{Log}(q) \rightarrow -\infty$. The initial conditions are $q(0) = 7000$, $p(0) = 10$.

The equations of motion obtained from the (12) are

$$\begin{aligned} \dot{q} &= -\frac{9}{2}p, \\ \dot{\beta}'_+ &= 2p'_+, \\ \dot{\beta}'_- &= 2p'_-, \\ \dot{p} &= -\frac{3(4\pi)^4}{k} q^{-1/3} \left(q \frac{\partial V(q, \beta'_+, \beta'_-)}{\partial q} - \frac{2}{3} \right), \\ \dot{p}'_+ &= -\frac{3(4\pi)^4}{k} q^{2/3} \frac{\partial V(q, \beta'_+, \beta'_-)}{\partial \beta'_+}, \\ \dot{p}'_- &= -\frac{3(4\pi)^4}{k} q^{2/3} \frac{\partial V(q, \beta'_+, \beta'_-)}{\partial \beta'_-}. \end{aligned} \quad (16)$$

In figure 5 and (6) we show the classical evolution obtained from (16).

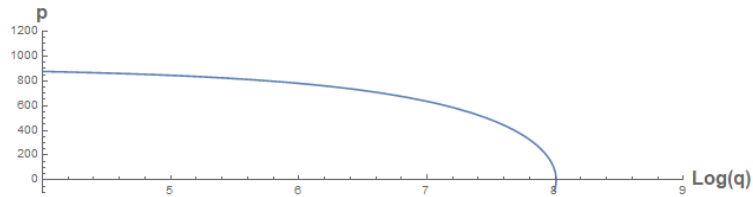


Figure 5: $\text{Log}(q)$ vs p plot. The initial conditions are $q(0) = 3000$, $p(0) = 10$, $\beta'_+ = -0.1$, $\beta'_- = 0$, $p'_+ = 0.1$, $p'_- = 0.1$.

3 Effective dynamics of the Mixmaster model

3.1 Effective momenta quantum mechanics

In usual quantum mechanics, the Schrödinger equation $\hat{H}\psi = E\psi$ determines the evolution of the system: all the information is encoded in the wave function, and classical variables are now operators. Within this Schrödinger representation, the concept of a single particle's position is absent, and also trajectories. It is possible, however, with a generalization of the Ehrenfest theorem, to obtain an effective description by means of a Hamiltonian $H_Q = \langle \hat{H} \rangle$, which depends on expectation values of observables and quantum dispersions (or momenta) [32]. Once this

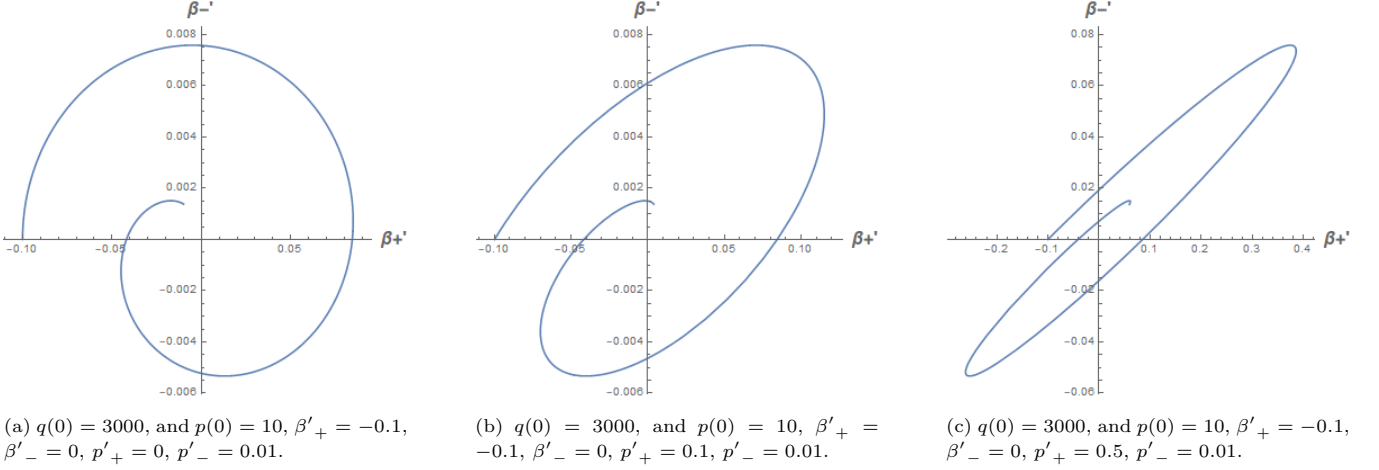


Figure 6: Classical evolution in the space (β'_+, β'_-) .

Hamiltonian is obtained, dynamical equations of motion can be obtained in the usual way through the following equation

$$\{\langle \hat{f} \rangle, \langle \hat{g} \rangle\} = \frac{1}{i\hbar} \langle [\hat{f}, \hat{g}] \rangle. \quad (17)$$

For one degree of freedom, these momenta are defined as

$$G^{a,b} := \langle (\hat{p} - \langle \hat{p} \rangle)^a (\hat{q} - \langle \hat{q} \rangle)^b \rangle_{\text{Weyl}}, \quad (18)$$

where $\langle \hat{q} \rangle$ and $\langle \hat{p} \rangle$ are the expectation values of position and momentum respectively, and $a + b \geq 2$. The legend Weyl means totally symmetrization [20]. The momenta $G^{a,b}$ obey a generalization of the Heisenberg uncertainty principle [18], that is

$$G^{2,0}G^{0,2} - (G^{1,1})^2 \geq \frac{\hbar^2}{4}. \quad (19)$$

The effective Hamiltonian H_Q is defined in the following way

$$H_Q = \sum_{a=0}^{\infty} \sum_{b=0}^{\infty} \frac{1}{a!b!} \frac{\partial^{a+b} H}{\partial p^a \partial q^b} G^{a,b}. \quad (20)$$

A general expression for k degrees of freedom for H_Q is [33]

$$H_Q = \sum_{a_1, b_1}^{\infty} \cdots \sum_{a_k, b_k}^{\infty} \frac{1}{a_1! b_1! \cdots a_k! b_k!} \frac{\partial^{a_1+b_1+\cdots+a_k+b_k} H}{\partial q_1^{a_1} \partial p_1^{b_1} \cdots \partial q_k^{a_k} \partial p_k^{b_k}} G^{a_1, b_1, \dots, a_k, b_k}. \quad (21)$$

Equations of motion are obtained from this effective Hamiltonian. For general systems there are an infinite number of momenta and, correspondingly, an infinite number of equations of motion, usually impossible to solve analytically, although consistent truncations can be implemented in order to obtain approximated solutions [34].

Analysis of this effective dynamics is done usually in a numerical way, for which initial conditions are required. We employ general squeezed states to determine such conditions, for example, for a Gaussian function ψ_σ

$$\psi_\sigma(q) = \frac{1}{\pi^{1/4} \sqrt{\sigma}} \exp \left\{ -\frac{(q - \langle q \rangle)^2}{2\sigma^2} + \frac{iq\langle p \rangle}{\hbar} \right\}, \quad (22)$$

we can readily obtain the initial values for quantum variables. For instance

$$G^{a,b} = \begin{cases} 2^{-(a+b)} \hbar^a \sigma^{b-a} \frac{a!b!}{(a/2)!(b/2)!}, & a \text{ and } b \text{ even} \\ 0, & \text{otherwise} \end{cases} \quad (23)$$

One can see that the initial momenta $G^{a,b}$ saturate the Heisenberg uncertainty relation

$$G^{2,0}G^{0,2} = \frac{\hbar^2}{4}.$$

In this effective formulation, the momenta scale as powers of \hbar , that is

$$G^{a,b} \propto \hbar^{\frac{(a+b)}{2}},$$

It is possible to obtain important modifications of the classical system considering only the second order terms [34].

On the other hand, the momenta $G^{a,b}$ form a set of non-canonical coordinates in the quantum phase state which complicates the canonical analysis of the system [35]. However, it is possible to generalize this effective method through a coordinate transform that allow us to rewrite the momenta in terms of pairs of canonical variables s_i, p_{s_i} and Casimir parameters [36]. These new coordinates encode all the quantum information of the system. The main advantage of this reformulation is that it avoids the truncation required by the momenta approach, and allows us to construct an effective potential [37]

$$V_{\text{All}}(q, s) = \frac{1}{8s^2} + \frac{1}{2}[V(q+s) + V(q-s)], \quad (24)$$

where $V(q)$ is the classical potential of the system. In general, for 3 degrees of freedom we have [38]

$$V_{\text{All}}(x_i, s_j) = \sum_{i=1}^3 \frac{U}{2s_i^2} + \frac{1}{8}[V(x_i+s_i) + V(x_i-s_i)]. \quad (25)$$

For a second order truncation in the momenta $G^{a,b}$ the coordinate transformation is

$$\begin{aligned} s &= \sqrt{G^{0,2}} \\ p_s &= \frac{G^{1,1}}{\sqrt{G^{0,2}}} \\ U &= G^{0,2}G^{2,0} - (G^{1,1})^2. \end{aligned} \quad (26)$$

where $\{s, p_s\} = 1$, and $\{s, U\} = \{p_s, U\} = 0$ [35].

3.2 Momenta effective dynamics

In order to analyze the effective evolution of anisotropies β_+, β_- , we use the Hamiltonian (10)

$$H_{IX} = \sqrt{p_x^2 + p_y^2 + \frac{3(4\pi)^2}{k^2} e^{4\alpha} V(x, y)}, \quad (27)$$

where the potential $V(x, y)$ is

$$V(x, y) = e^{-8x} - 4e^{-2x} \cosh(2\sqrt{3}y) + 2e^{4x} [\cosh(4\sqrt{3}y) - 1]. \quad (28)$$

We have rewritten (for simplicity and to facilitate the numerical application of the method) $\beta_+ \rightarrow x, \beta_- \rightarrow y, p_+ \rightarrow p_x$, and $p_- \rightarrow p_y$.

Using the Hamiltonian (27), and truncating to second order in momenta the equation (21), we obtain the following expression

$$\begin{aligned} H_{QIX} &= H_{IX} + (H_{IX}^{-1} - p_x^2 H_{IX}^{-3}) G^{0200} + (H_{IX}^{-1} - p_y^2 H_{IX}^{-3}) G^{0002} + \eta(\alpha) \left[2 \frac{\partial}{\partial x} (g_1(x, y) H_{IX}^{-1}) G^{2000} \right. \\ &+ \left. 2\sqrt{3} \frac{\partial}{\partial y} (g_2(x, y) H_{IX}^{-1}) G^{0020} - \frac{4p_x}{H_{IX}^3} g_1(x, y) G^{1100} - \frac{4\sqrt{3}p_y}{H_{IX}^3} g_2(x, y) G^{0011} \right]. \end{aligned} \quad (29)$$

The functions $g_1(x, y)$, $g_2(x, y)$, and $\eta(\alpha)$ are as follows

$$\begin{aligned}
g_1(x, y) &= -e^{-8x} + e^{-2x} \cosh(2\sqrt{3}y) + e^{4x} \left(\cosh(4\sqrt{3}y) - 1 \right) \\
g_2(x, y) &= -e^{-2x} \sinh(2\sqrt{3}y) + e^{4x} \sinh(4\sqrt{3}y), \\
\eta(\alpha) &= \frac{3(4\pi)^2}{k^2} e^{4\alpha},
\end{aligned} \tag{30}$$

and the momenta for two degrees of freedom is given by

$$G^{abcd} := \langle (\hat{p}_x - \langle \hat{p}_x \rangle)^a (\hat{x} - \langle \hat{x} \rangle)^b (\hat{p}_y - \langle \hat{p}_y \rangle)^c (\hat{y} - \langle \hat{y} \rangle)^d \rangle_{\text{Weyl}}. \tag{31}$$

The equations of motion for the classical variables are

$$\begin{aligned}
\dot{x} &= \frac{p_x}{H_{IX}} - 2p_x \eta(\alpha) \frac{\partial}{\partial x} (g_1(x, y) H_{IX}^{-3}) G^{2000} - 4\eta(\alpha) g_1(x, y) \frac{\partial}{\partial p_x} (p_x H_{IX}^{-3}) G^{1100} \\
&+ \frac{1}{2} \frac{\partial}{\partial p_x} (H_{IX}^{-1} - p_x^2 H_{IX}^{-3}) G^{0200} + 2\sqrt{3}\eta(\alpha) \frac{\partial^2}{\partial p_x \partial y} (g_2(x, y) H_{IX}^{-1}) G^{0020} \\
&- 4\sqrt{3}p_y \eta(\alpha) \frac{\partial}{\partial p_x} (H_{IX}^{-3}) g_2(x, y) G^{0011} + \frac{1}{2} \frac{\partial}{\partial p_x} (H_{IX}^{-1} - p_y^2 H_{IX}^{-3}) G^{0002}, \\
\dot{y} &= \frac{p_y}{H_{IX}} + 2\eta(\alpha) \frac{\partial^2}{\partial x \partial p_y} (g_1(x, y) H_{IX}^{-1}) G^{2000} - 4p_x \eta(\alpha) \frac{\partial}{\partial p_y} (g_1(x, y) H_{IX}^{-3}) G^{1100} \\
&+ \frac{1}{2} \frac{\partial}{\partial p_y} (H_{IX}^{-1} - p_x^2 H_{IX}^{-3}) G^{0200} + 2\sqrt{3}\eta(\alpha) \frac{\partial^2}{\partial p_x \partial y} (g_2(x, y) H_{IX}^{-1}) G^{0020} \\
&+ \frac{\partial}{\partial y} (H_{IX}^{-1} - p_y^2 H_{IX}^{-3}) G^{0011} + \frac{1}{2} \frac{\partial}{\partial p_y} (H_{IX}^{-1} - p_y^2 H_{IX}^{-3}) G^{0002}, \\
\dot{p}_x &= -4\eta(\alpha) g_1(x, y) H_{IX}^{-1} - 2\eta(\alpha) \frac{\partial^2}{\partial x^2} (g_1(x, y) H_{IX}^{-1}) G^{2000} - 4\eta(\alpha) \frac{\partial^2}{\partial x \partial p_x} (g_1(x, y) H_{IX}^{-1}) G^{1100} \\
&- \frac{1}{2} \frac{\partial}{\partial x} (H_{IX}^{-1} - p_x^2 H_{IX}^{-3}) G^{0200} - 2\sqrt{3}\eta(\alpha) \frac{\partial^2}{\partial x \partial y} (g_2(x, y) H_{IX}^{-1}) G^{0020} \\
&+ 4\sqrt{3}p_y \eta(\alpha) \frac{\partial}{\partial x} (g_2(x, y) H_{IX}^{-3}) G^{0011} - \frac{1}{2} \frac{\partial}{\partial x} (H_{IX}^{-1} - p_y^2 H_{IX}^{-3}) G^{0002}, \\
\dot{p}_y &= -4\sqrt{3}\eta(\alpha) g_2(x, y) H_{IX}^{-1} - 2\eta(\alpha) \frac{\partial^2}{\partial x \partial y} (g_1(x, y) H_{IX}^{-1}) G^{2000} + 4p_x \eta(\alpha) \frac{\partial}{\partial y} (g_1(x, y) H_{IX}^{-3}) G^{1100} \\
&- \frac{1}{2} \frac{\partial}{\partial y} (H_{IX}^{-1} - p_x^2 H_{IX}^{-3}) G^{0200} - 2\sqrt{3}\eta(\alpha) \frac{\partial^3}{\partial y^3} (g_2(x, y) H_{IX}^{-1}) G^{0020} \\
&- 4\sqrt{3}\eta(\alpha) \frac{\partial^2}{\partial y \partial p_y} (g_2(x, y) H_{IX}^{-1}) G^{0011} - \frac{1}{2} \frac{\partial}{\partial y} (H_{IX}^{-1} - p_y^2 H_{IX}^{-3}) G^{0002},
\end{aligned} \tag{32}$$

and for the momenta,

$$\begin{aligned}
\dot{G}^{2000} &= \frac{8p_x}{H_{IX}^3} \eta(\alpha) g_1(x, y) G^{2000} - 2 (H_{IX}^{-1} - p_x^2 H_{IX}^{-3}) G^{1100} \\
\dot{G}^{1100} &= 4\eta(\alpha) \frac{\partial}{\partial x} (g_1(x, y) H_{IX}^{-1}) G^{2000} - (H_{IX}^{-1} - p_x^2 H_{IX}^{-3}) G^{0200} \\
\dot{G}^{0200} &= 8\eta(\alpha) \frac{\partial}{\partial x} (g_1(x, y) H_{IX}^{-1}) G^{1100} - \frac{8p_x}{H_{IX}^3} \eta(\alpha) g_1(x, y) G^{0200} \\
\dot{G}^{0020} &= \frac{8\sqrt{3}p_y}{H_{IX}^3} \eta(\alpha) g_2(x, y) G^{0020} - 2 (H_{IX}^{-1} - p_y^2 H_{IX}^{-3}) G^{0011} \\
\dot{G}^{0011} &= 4\sqrt{3}\eta(\alpha) \frac{\partial}{\partial y} (g_2(x, y) H_{IX}^{-1}) G^{0020} - (H_{IX}^{-1} - p_y^2 H_{IX}^{-3}) G^{0002} \\
\dot{G}^{0002} &= 8\sqrt{3}\eta(\alpha) \frac{\partial}{\partial y} (g_2(x, y) H_{IX}^{-1}) G^{0011} - \frac{8\sqrt{3}p_y}{H_{IX}^3} \eta(\alpha) g_2(x, y) G^{0002}.
\end{aligned} \tag{33}$$

These are two sets of coupled and highly non-linear equations providing the evolution of the quantum modified anisotropies, we employ a numerical method to obtain the dynamics of this system, and its trajectories.

To obtain the dynamics of classical variables (q, β'_+, β'_-) and their corresponding momenta, we use the Hamiltonian (12). To this end we construct H_Q using equation (21) with three degrees of freedom.

Up to second order in momenta we obtain the following

$$H_Q = \mathcal{K} - \frac{9}{4}A + D + G + \frac{1}{2} \frac{\partial^2 \mathcal{K}}{\partial q^2} B + \frac{1}{2} \frac{\partial^2 \mathcal{K}}{\partial \beta'^2_+} E + \frac{1}{2} \frac{\partial^2 \mathcal{K}}{\partial \beta'^2_-} H, \quad (34)$$

where the momenta for three degrees of freedom is defined as follows

$$G^{abcdef} := \langle (\hat{p} - \langle \hat{p} \rangle)^a (\hat{q} - \langle \hat{q} \rangle)^b (\hat{p}_+ - \langle \hat{p}_+ \rangle)^c (\hat{\beta}'_+ - \langle \hat{\beta}'_+ \rangle)^d (\hat{p}_- - \langle \hat{p}_- \rangle)^e (\hat{\beta}'_- - \langle \hat{\beta}'_- \rangle)^f \rangle_{\text{Weyl}}. \quad (35)$$

In the table (1), the second order momenta are summarized

$A = G^{200000}$	$D = G^{002000}$	$G = G^{000020}$
$B = G^{020000}$	$E = G^{000200}$	$H = G^{000002}$
$C = G^{110000}$	$F = G^{001100}$	$J = G^{000011}$

Table 1: Second order momenta for three degrees of freedom.

The equations of motion obtained from (34) form a system of fifteen coupled equations that describes the dynamics of the Mixmaster model. Equations for the classical variables are

$$\begin{aligned} \dot{p} &= -\frac{3(4\pi)^4}{8\pi} \frac{\partial}{\partial q} \left(q^{2/3} V(q, \beta'_+, \beta'_-) \right) - \frac{1}{2} \frac{\partial^3 \mathcal{K}}{\partial q^3} B - \frac{1}{2} \frac{\partial^3 \mathcal{K}}{\partial q \partial \beta'^2_+} E - \frac{1}{2} \frac{\partial^3 \mathcal{K}}{\partial q \partial \beta'^2_-} H, \\ \dot{p}'_+ &= -\frac{3(4\pi)^4 q^{2/3}}{8\pi} \frac{\partial}{\partial \beta'_+} V(q, \beta'_+, \beta'_-) - \frac{1}{2} \frac{\partial^3 \mathcal{K}}{\partial \beta'_+ \partial q^2} B - \frac{1}{2} \frac{\partial^3 \mathcal{K}}{\partial \beta'^3_+} E - \frac{1}{2} \frac{\partial^3 \mathcal{K}}{\partial \beta'_+ \partial \beta'^2_-} H, \\ \dot{p}'_- &= -\frac{3(4\pi)^4 q^{2/3}}{8\pi} \frac{\partial}{\partial \beta'_-} V(q, \beta'_+, \beta'_-) - \frac{1}{2} \frac{\partial^3 \mathcal{K}}{\partial \beta'_- \partial q^2} B - \frac{1}{2} \frac{\partial^3 \mathcal{K}}{\partial \beta'_- \partial \beta'^2_+} E - \frac{1}{2} \frac{\partial^3 \mathcal{K}}{\partial \beta'^3_-} H, \\ \dot{q} &= -\frac{9}{2} p, \\ \dot{\beta}'_+ &= 2p'_+, \\ \dot{\beta}'_- &= 2p'_-, \end{aligned} \quad (36)$$

while for quantum variables we have

$$\begin{aligned} \dot{A} &= -2 \frac{\partial^2 \mathcal{K}}{\partial q^2} C, & \dot{D} &= -2 \frac{\partial^2 \mathcal{K}}{\partial \beta'^2_+} F, & \dot{G} &= -2 \frac{\partial^2 \mathcal{K}}{\partial \beta'^2_-} J, \\ \dot{B} &= -9C, & \dot{E} &= 4F, & \dot{H} &= 4J, \\ \dot{C} &= -\frac{9}{2} A - \frac{\partial^2 \mathcal{K}}{\partial q^2} B, & \dot{F} &= 2D - \frac{\partial^2 \mathcal{K}}{\partial \beta'^2_+} E, & \dot{J} &= 2G - \frac{\partial^2 \mathcal{K}}{\partial \beta'^2_-} H. \end{aligned} \quad (37)$$

3.3 Canonical effective dynamics

Using equations (12) and (25), we construct the effective Hamiltonian \mathcal{K}_{all} defined as

$$\mathcal{K}_{all} = -\frac{9}{4}(p^2 + p_1^2) + (p'^2_+ + p_2^2) + (p'^2_- + p_3^2) + V_{\text{eff}}, \quad (38)$$

where

$$V_{\text{eff}} = \left(\frac{s_2^2 s_3^2 + s_1^2 s_3^2 + s_1^2 s_2^2}{8s_1^2 s_2^2 s_3^2} \right) + \frac{3(4\pi)^4}{8k} \left[(q + s_1)^{2/3} V_{\mathcal{H}^+} + (q - s_1)^{2/3} V_{\mathcal{H}^-} \right], \quad (39)$$

and

$$V_{\mathcal{H}^\pm} = e^{-\frac{8(\beta'_+ \pm s_2)}{(q \pm s_1)}} - 4e^{-\frac{2(\beta'_+ \pm s_2)}{(q \pm s_1)}} \cosh \left(\frac{2\sqrt{3}(\beta'_- \pm s_3)}{(q \pm s_1)} \right) + 2e^{\frac{4(\beta'_+ \pm s_2)}{(q \pm s_1)}} \left[\cosh \left(\frac{4\sqrt{3}(\beta'_- \pm s_3)}{(q \pm s_1)} \right) - 1 \right]. \quad (40)$$

In this scheme, the new pairs of canonical variables (s_i, p_{s_i}) encode all the quantum information of the system. The equations of motion obtained from this effective Hamiltonian are

$$\begin{aligned}
\dot{q} &= -\frac{9}{2}p, & \dot{p} &= -\frac{1}{8}\frac{\partial}{\partial q}(V_{\mathcal{H}}^+ + V_{\mathcal{H}}^-), \\
\dot{\beta}'_+ &= 2p'_+, & \dot{p}'_+ &= -\frac{1}{8}\frac{\partial}{\partial \beta'_+}(V_{\mathcal{H}}^+ + V_{\mathcal{H}}^-), \\
\dot{\beta}'_- &= 2p'_-, & \dot{p}'_- &= -\frac{1}{8}\frac{\partial}{\partial \beta'_-}(V_{\mathcal{H}}^+ + V_{\mathcal{H}}^-), \\
\dot{s}_1 &= -\frac{9}{2}p_1, & \dot{p}_1 &= \frac{1}{4s_1^3} - \frac{1}{8}\frac{\partial}{\partial s_1}(V_{\mathcal{H}}^+ + V_{\mathcal{H}}^-), \\
\dot{s}_2 &= 2p_2, & \dot{p}_2 &= \frac{1}{4s_2^3} - \frac{1}{8}\frac{\partial}{\partial s_2}(V_{\mathcal{H}}^+ + V_{\mathcal{H}}^-), \\
\dot{s}_3 &= 2p_3, & \dot{p}_3 &= \frac{1}{4s_3^3} - \frac{1}{8}\frac{\partial}{\partial s_3}(V_{\mathcal{H}}^+ + V_{\mathcal{H}}^-).
\end{aligned} \tag{41}$$

4 Numerical solution.

For one degree of freedom, the momenta $G^{a,b}$ are defined as

$$G^{a,b} := \langle (\hat{p} - p)^a (\hat{q} - q)^b \rangle_{\text{Weyl}}$$

where $p := \langle \hat{p} \rangle$, and $q := \langle \hat{q} \rangle$. Using the Gaussian wave function (22), the initial conditions for the momenta $G^{a,b}$ can be determined. For instance, the initial condition for $G^{2,0}$ is

$$\begin{aligned}
G^{2,0} &= \langle \psi_\sigma^*(\hat{q}) | (\hat{p} - p)^2 | \psi_\sigma(\hat{q}) \rangle \\
&= \eta \int_{-\infty}^{\infty} e^{-\frac{(\hat{q}-\langle \hat{q} \rangle)^2}{\sigma^2}} (\zeta - 2\langle \hat{q} \rangle + \hat{q}^2) d\hat{q} \\
&= \frac{\hbar^2}{2\sigma^2},
\end{aligned} \tag{42}$$

where $\eta = \frac{-\hbar^2}{\sqrt{\pi}\sigma^5}$, and $\zeta = \langle \hat{q} \rangle^2 - \sigma^2$ are constants. Following a similar procedure, the second order initial values for momenta are

$$\begin{aligned}
G^{2,0} &= \frac{\hbar^2}{2\sigma^2}, \\
G^{1,1} &= 0, \\
G^{0,2} &= \frac{\sigma^2}{2}.
\end{aligned} \tag{43}$$

On the other hand, for two degrees of freedom the momenta $G^{a,b,c,d}$ are defined as

$$\begin{aligned}
G^{a,b,c,d} &:= \langle (\hat{p}_1 - p_1)^a (\hat{q}_1 - q_1)^b \\
&\quad \times (\hat{p}_2 - p_2)^c (\hat{q}_2 - q_2)^d \rangle_{\text{Weyl}},
\end{aligned}$$

where $p_1 := \langle \hat{p}_1 \rangle$, $q_1 := \langle \hat{q}_1 \rangle$, $p_2 := \langle \hat{p}_2 \rangle$, and $q_2 := \langle \hat{q}_2 \rangle$. Employing a similar procedure for the one degree of freedom case, the initial conditions for the second order moments, with two degree of freedom G^{abcd} are

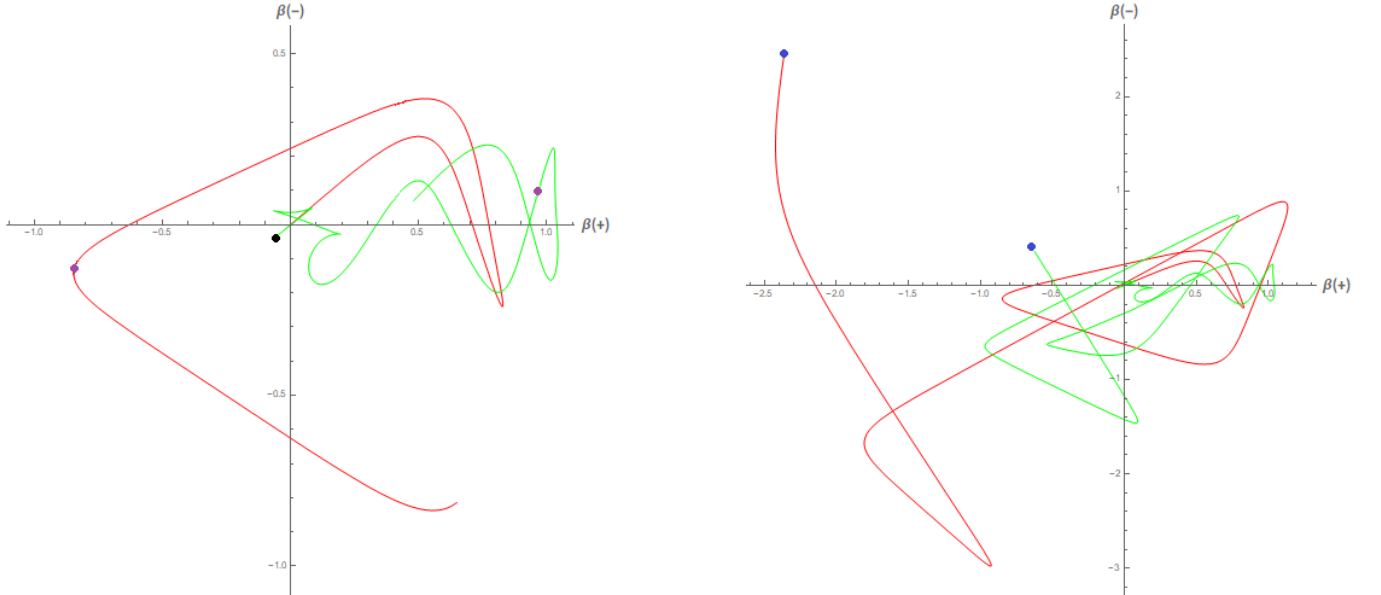
$$\begin{aligned}
G^{2000} &= G^{0020} = \frac{\hbar^2}{2\sigma^2}, \\
G^{1100} &= G^{0011} = 0, \\
G^{0200} &= G^{0002} = \frac{\sigma^2}{2}.
\end{aligned} \tag{44}$$

For three degrees of freedom we get

$$\begin{aligned}
G^{200000} &= G^{002000} = G^{000020} = \frac{\hbar^2}{2\sigma^2}, \\
G^{110000} &= G^{001100} = G^{000011} = 0, \\
G^{020000} &= G^{000200} = G^{000002} = \frac{\sigma^2}{2}.
\end{aligned} \tag{45}$$

The set of equations (32) and (33) describes the dynamics of anisotropies and quantum momenta of the Mixmaster model. The coupling between both kinds of variables generates a quantum backreaction that modifies the classical evolution of the system, which we explore now.

We employ initial conditions (44) to generate, numerically, the evolution of the system. In figure 7 we show the modification of the classical trajectories (red) due the quantum effects. In figure 7a the black dot denotes the starting point of both trajectories classical and effective (green), while the purple dots correspond to both trajectories at the same time. However, unlike the straight line behavior of classical trajectories near the initial singularity as $|\beta_{\pm}| \rightarrow \infty$, as discussed in section 2, and shown in figure 2a, the interaction of the quantum momenta with the classical system increases the changes in direction of the trajectory for the semiclassical particle at early times, drastically changing its linear behavior. Figure 7b represents the same trajectories for different evolution times.

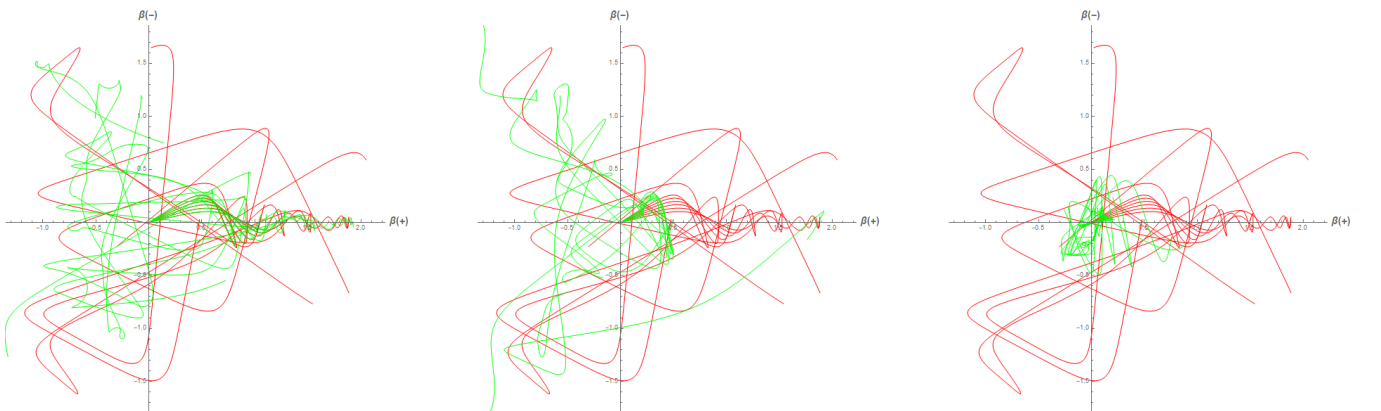


(a) Classical (red) and effective evolution (green) for anisotropies up to $t = 6$.

(b) Classical (red) and effective evolution (green) for the anisotropies up to $t = 20$.

Figure 7: Comparison between classical (red) and effective evolution (green) for the anisotropies of the Mixmaster model. The initial singularity corresponds to $|\beta_{\pm}| \rightarrow \infty$. The dots represent the position at equal times. The initial conditions are $\beta_+(0) = 0$, $\beta_- = 0$, $p_+ = 100$, and $p_- = 64$, and those of eq.(43) for the momenta with $\sigma = 2.2$.

In figure 8 we show a comparison between several classical and semiclassical trajectories, displaying chaotic behavior [17].



(a) Classical and quantum evolution for $\sigma = 0.08$.

(b) Classical and quantum evolution for $\sigma = 0.6$.

(c) Classical and quantum evolution for $\sigma = 2.6$.

Figure 8: Comparison between classical (Red) and effective evolution (Green) for the anisotropies of the Mixmaster model. The initial conditions for the classical model are $\beta_+(0) = 0$, $\beta_- = 0$, $p_+ = 100$, and $p_- = 8i$ (where $i = 1, 2, 3, \dots, 10$ corresponds to a different trajectory). The initial conditions for the effective evolution are $\beta_+(0) = 0$, $\beta_- = 0$, $p_+ = 100$, $p_- = 8i$ and those of eq.(43) for the momenta.

Additionally in Figure (9) we show the classical and semiclassical evolution in the phase space diagram $(p, \text{Log}(q))$, where q is related to the scale factor through $q = \sqrt{a}$. In this diagram $t = 0$ occurs when $\text{Log}(q) \rightarrow -\infty$, that is, $a \rightarrow 0$. The classical trajectory (blue) displays $\text{Log}(q) \rightarrow -\infty$, that is, it contains the initial singularity, while the effective trajectories in momenta (black) and canonical potential (purple) $|\text{Log}(q)| < \infty$, thus removing the initial singularity.

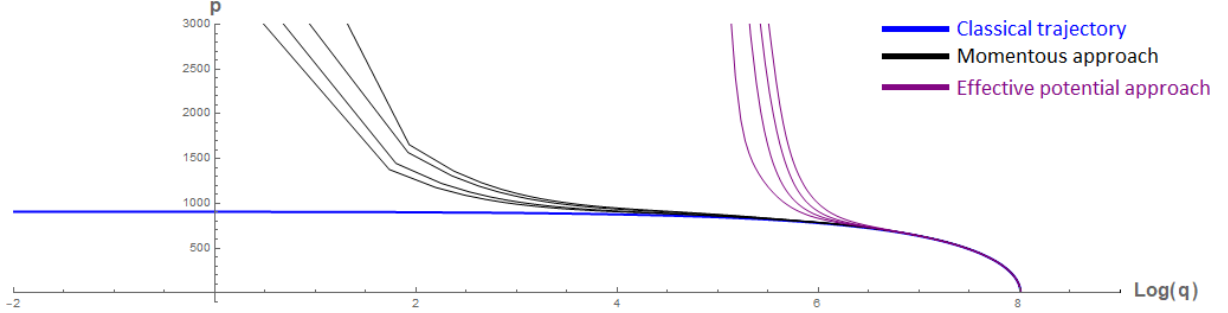


Figure 9: Phase space diagram of $\text{Log}(q)$ and p . Unlike the classical evolution (blue), which contains the initial singularity at $t=0$, the effective trajectories avoid it because $|\text{Log}(q)| < \infty$. The different trajectories corresponds to a different values of σ . The initial conditions are $q(0) = 0.1$, $p(0) = 1200$, and $\sigma = 6, \sigma = 8, \sigma = 10$, and $\sigma = 12$.

In figure 10 we show classical and semiclassical trajectories within the all order potential method for different initial conditions of quantum variables s_i .

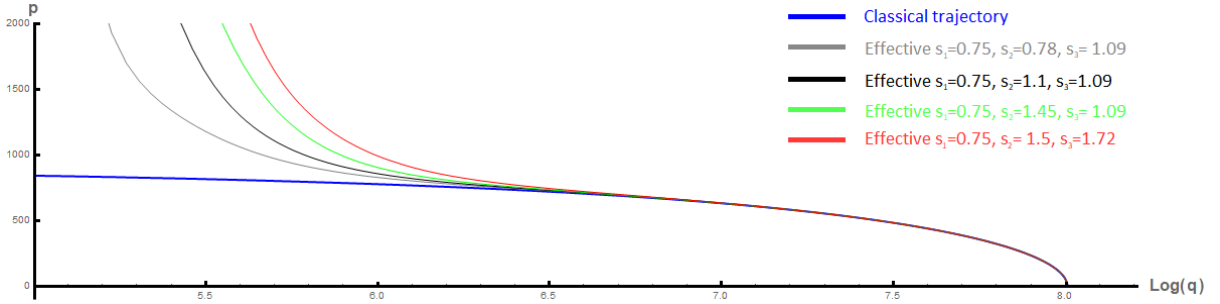


Figure 10: Comparison between the classical evolution (blue) and semiclassical with effective potential in the phase space diagram $\text{Log}(q)$ and p . For the classical trajectory $\text{Log}(q) \rightarrow -\infty$, while in the semiclassical ones $|\text{Log}(q)| < \infty$, removing the initial singularity. The initial conditions are $q(0) = 0.1$, $p(0) = 1200$, and $\sigma = 6, \sigma = 8, \sigma = 10, \sigma = 12$.

5 Conclusions

In this article the quantum Mixmaster model was analyzed in a semiclassical setting, finding important differences with respect to the classical model. In particular, by studying semiclassical trajectories describing the evolution of anisotropies we show that the initial singularity is avoided as a result of quantum back reaction.

In the classical Mixmaster model, the universe is subject to a time dependent potential evolving in a space of anisotropies, and has a singularity at $t = 0$, where the interaction with the potential walls is less frequent. We apply a canonical transformation in the classical Hamiltonian to obtain an expression more suitable to implement the effective analysis for the quantum model. Under this formulation it is possible to make a direct comparison between the quantum corrected behavior and that of the classical model by means of effective trajectories.

The behavior displayed by the quantum model derived from the effective Hamiltonian (29) shows that, although the classical evolution is drastically modified due to quantum backreaction through quantum momenta, it retains its chaotic behaviour regardless of initial conditions taken into account, in agreement with recent similar studies [17].

In the classical evolution, the initial singularity is reached as $|\beta_{\pm}| \rightarrow \infty$. Because the trajectory is a straight line in that case, it means that the particle does not interact with the classical potential near $t = 0$. In the quantum regime, the interaction of the particle with the potential is stronger due to back reaction, generating more dispersions, and preventing the particle from reaching $|\beta_{\pm}| \rightarrow \infty$, thus avoiding the singularity.

After performing a canonical transformation we obtain an effective Hamiltonian (34) in terms of anisotropies, the scale factor a and their quantum momenta. Unlike the classical behaviour, the effective evolution shows that quantum variables impose a minimum lower bound on the volume of the universe, as shown in figure 9, i.e, the initial singularity is removed.

Finally, the evolution obtained from the canonical Hamiltonian (38) also displays a singularity avoidance (Figure 10). The Hamiltonian (34) is used to perform an effective analysis based in momenta up to second order G^{abcd} (Figure 9), while the Hamiltonian (38) is employed to generate the effective dynamics of the system in terms of canonical variables (s_i, p_{s_i}) and effective potential.

The main difference between the momenta and the canonical potential descriptions is the need to truncate the dynamical system for the former. This in turn derives in that the minimum value for a is different in each case, being larger when the canonical potential is used. For the present analysis both descriptions were possible and, as shown, both give similar results; however, there are systems for which one description cannot be applied, but the other is.

In our analysis we have applied a canonical transformation that renders the effective Hamiltonian (7) explicitly as kinetic plus potential terms. This transformation allows the application of the generalized potential method, and with this obtain the evolution of the scale factor and the anisotropies of the system from the same system of equations, which is not possible in the $G^{a,b}$ formulation. There exist similar effective analysis of the Mixmaster model focusing on the study of anisotropies [22, 17, 31].

Our study can be used to generalize the analysis of anisotropic cosmological models into inhomogeneous models, where we expect to obtain interesting results in this effective description [39, 40, 21].

References

- [1] Claus Kiefer, Nick Kwidzinski, and Włodzimierz Piechocki. On the dynamics of the general bianchi ix spacetime near the singularity. *The European Physical Journal C*, 78:1–10, 2018.
- [2] Alexey S Koshelev, João Marto, and Anupam Mazumdar. Towards resolution of anisotropic cosmological singularity in infinite derivative gravity. *arXiv preprint arXiv:1803.07072*, 2018.
- [3] Alexey Toporensky and Shinji Tsujikawa. Nature of singularities in anisotropic string cosmology. *Physical Review D*, 65(12):123509, 2002.
- [4] Bijan Saha. Anisotropic cosmological models with a perfect fluid and a λ term. *Astrophysics and space science*, 302:83–91, 2006.
- [5] Burak Himmetoglu, Carlo R Contaldi, and Marco Peloso. Instability of anisotropic cosmological solutions supported by vector fields. *Physical review letters*, 102(11):111301, 2009.
- [6] Hans Ringström. The bianchi ix attractor. In *Annales Henri Poincaré*, volume 2, pages 405–500. Springer, 2001.
- [7] Włodzimierz Piechocki. Quantum chaos of the belinski–khalatnikov–lifshitz scenario.
- [8] Joshua Ritchie. Bianchi i ‘asymptotically kasner’ solutions of the einstein scalar field equations. *Classical and Quantum Gravity*, 39(13):135007, 2022.
- [9] Ana Alonso-Serrano, David Brizuela, and Sara F Uria. Quantum kasner transition in a locally rotationally symmetric bianchi ii universe. *Physical Review D*, 104(2):024006, 2021.
- [10] Eleonora Giovannetti and Giovanni Montani. Polymer representation of the bianchi ix cosmology in the misner variables. *Physical Review D*, 100(10):104058, 2019.
- [11] Charles W Misner. The mixmaster cosmological metrics. *Deterministic Chaos in General Relativity*, pages 317–328, 1994.
- [12] Neil J Cornish and Janna J Levin. The mixmaster universe is chaotic. *Physical Review Letters*, 78(6):998, 1997.
- [13] John D Barrow. Chaotic behaviour in general relativity. *Physics Reports*, 85(1):1–49, 1982.
- [14] Andrew Zardecki. Modeling in chaotic relativity. *Physical Review D*, 28(6):1235, 1983.
- [15] Johannes Brunnemann and Thomas Thiemann. On (cosmological) singularity avoidance in loop quantum gravity. *Classical and Quantum Gravity*, 23(5):1395, 2006.
- [16] Orchidea Maria Lecian, Giovanni Montani, and Riccardo Moriconi. Semiclassical and quantum behavior of the mixmaster model in the polymer approach. *Physical Review D*, 88(10):103511, 2013.
- [17] Martin Bojowald, David Brizuela, Paula Calizaya Cabrera, and Sara F Uria. The chaotic behavior of the bianchi ix model under the influence of quantum effects. *arXiv preprint arXiv:2307.00063*, 2023.

- [18] Martin Bojowald and Aureliano Skirzewski. Effective equations of motion for quantum systems. *Reviews in Mathematical Physics*, 18(07):713–745, 2006.
- [19] L Aragón-Muñoz, G Chacón-Acosta, and H Hernandez-Hernandez. Effective quantum tunneling from a semi-classical momentous approach. *International Journal of Modern Physics B*, 34(29):2050271, 2020.
- [20] Martin Bojowald, David Brizuela, Hector H Hernández, Michael J Koop, and Hugo A Morales-Técotl. High-order quantum back-reaction and quantum cosmology with a positive cosmological constant. *Physical Review D*, 84(4):043514, 2011.
- [21] David Brizuela and Unai Muniain. A moment approach to compute quantum-gravity effects in the primordial universe. *Journal of Cosmology and Astroparticle Physics*, 2019(04):016, 2019.
- [22] David Brizuela and Sara F Uria. Semiclassical study of the mixmaster model: The quantum kasner map. *Physical Review D*, 106(6):064051, 2022.
- [23] Marco Valerio Battisti and Giovanni Montani. The mixmaster universe in a generalized uncertainty principle framework. *Physics Letters B*, 681(2):179–184, 2009.
- [24] Jun-Qi Guo, Daoyan Wang, and Andrei V Frolov. Spherical collapse in $f(R)$ gravity and the belinskii-khalatnikov-lifshitz conjecture. *Physical Review D*, 90(2):024017, 2014.
- [25] J Mark Heinzle, Claes Uggla, and Woei Chet Lim. Spike oscillations. *Physical Review D*, 86(10):104049, 2012.
- [26] Abhay Ashtekar, Adam Henderson, and David Sloan. Hamiltonian formulation of the belinskii-khalatnikov-lifshitz conjecture. *Physical Review D*, 83(8):084024, 2011.
- [27] Charles W Misner. Mixmaster universe. *Physical Review Letters*, 22(20):1071, 1969.
- [28] Riccardo MORICONI, Salvatore CAPOZZIELLO, and Giovanni MONTANI. Dynamical systems in quantum cosmology.
- [29] Kip S Thorne, Charles W Misner, and John Archibald Wheeler. *Gravitation*. Freeman, 2000.
- [30] Michael P Ryan and Lawrence C Shepley. *Homogeneous relativistic cosmologies*. Princeton University Press, 2015.
- [31] Jaime de Cabo Martín. Mixmaster universe: semiclassical dynamics and inflation from bouncing. *arXiv e-prints*, pages arXiv–2302, 2023.
- [32] Martin Bojowald. *Quantum cosmology: a fundamental description of the universe*, volume 835. Springer Science & Business Media, 2011.
- [33] Hector H Hernandez Hernandez and Carlos R Javier Valdez. Semiclassical trajectories in the double-slit experiment. *arXiv preprint arXiv:2106.03280*, 2021.
- [34] Martin Bojowald. Quantum cosmology: effective theory. *Classical and Quantum Gravity*, 29(21):213001, 2012.
- [35] Ding Ding. Effective methods in cosmology and gravity. 2022.
- [36] Bekir Baytaş, Martin Bojowald, and Sean Crowe. Faithful realizations of semiclassical truncations. *Annals of Physics*, 420:168247, 2020.
- [37] Bekir Baytaş, Martin Bojowald, and Sean Crowe. Effective potentials from semiclassical truncations. *Physical Review A*, 99(4):042114, 2019.
- [38] Bekir Baytaş, Martin Bojowald, and Sean Crowe. Canonical tunneling time in ionization experiments. *Physical Review A*, 98(6):063417, 2018.
- [39] Martin Bojowald and Ding Ding. Canonical description of cosmological backreaction. *Journal of Cosmology and Astroparticle Physics*, 2021(03):083, 2021.
- [40] Martin Bojowald and Freddy Hancock. Quasiclassical model of inhomogeneous cosmology. *Classical and Quantum Gravity*, 2022.